Atmos. Chem. Phys. Discuss., https://doi.org/10.5194/acp-2018-1216
Manuscript under review for journal Atmos. Chem. Phys.
Discussion started: 27 November 2018

Atmospheric Chemistry and Physics Discussions

Integration of Airborne and Ground Observations of Nitryl Chloride in the Seoul Metropolitan Area and the Implications on Regional Oxidation Capacity During KORUS-AQ 2016

Daun Jeong[1], Roger Seco[1], Dasa Gu[1], Youngro Lee[2], Benjamin A. Nault[3,4], Christoph J. Knote[5], Tom Mcgee[6], John T. Sullivan[6], Jose L. Jimenez[3,4], Pedro Campuzano-Jost[3,4], Donald R. Blake[1], Dianne Sanchez[1], Alex B. Guenther[1], David Tanner[2], L. Gregory Huey[2], Russell Long[7], Bruce E. Anderson[8], Samuel R. Hall[9], Kirk Ullmann[9], Hye-jung Shin[10], Scott C. Herndon[11], YoungJae Lee[10], Danbi Kim[10], Joonyoung Ahn[10], and Saewung Kim[1]

[1]Department of Earth System Science, University of California, Irvine, Irvine, CA, USA
[2]School of Earth and Atmospheric Sciences, Georgia Institute of Technology, Atlanta, GA, USA
[3]Cooperative Institute for Research in Environmental Sciences, University of Colorado, Boulder, CO, USA
[4]Department of Chemistry, University of Colorado, Boulder, CO, USA
[5]Meteorologisches Institut, Ludwig-Maximilians-Universität München, München, Germany
[6]Chemistry and Dynamics Laboratory, NASA Goddard Space Flight Center, Greenbelt, MD, USA
[7]Office of Research and Development, U.S. EPA, Research Triangle Park, NC, USA
[8]NASA Langley Research Center, Hampton, VA, USA
[9]National Center for Atmospheric Research, Boulder, CO, USA
[10]National Institute of Environmental Research, Incheon, South Korea
[11]Aerodyne Research Inc., Billerica, MA, United States

Correspondence: Saewung Kim (saewung.kim@uci.edu)

Atmos. Chem. Phys. Discuss., https://doi.org/10.5194/acp-2018-1216
Manuscript under review for journal Atmos. Chem. Phys.
Discussion started: 27 November 2018

Atmospheric Chemistry and Physics Discussions

Abstract. Nitryl chloride ($ClNO_2$) is a radical reservoir species that releases chlorine radicals upon photolysis. An integrated analysis of the impact of $ClNO_2$ on regional photochemistry in the Seoul Metropolitan Area (SMA) during the Korean-United States-Air Quality (KORUS-AQ) 2016 field campaign is presented. Comprehensive multiplatform observations were conducted aboard the NASA DC-8 and at two ground sites (Olympic Park, OP; Taehwa Research Forest, TRF), representing an urbanized area and a forested region downwind, respectively. The overall diurnal variations of $ClNO_2$ in both sites appeared similar but the night time variation were systematically different. For about half of the observation days at the OP site the level of $ClNO_2$ increased at sunset but rapidly decreased at around midnight. On the other hand, high levels were sustained throughout the night at the TRF site. Significant levels of $ClNO_2$ were sustained at both sites for 4-5 hours after sunrise. Airborne observations, box model calculations, and back trajectory analysis consistently show that these high levels of $ClNO_2$ in the morning are likely due to the transport of air masses within the boundary layer. Box model results show that chlorine radical initiated chemistry can impact the regional photochemistry by elevating net ozone production rate up to $\sim$ 25 % in the morning.

1 Introduction

Nitryl chloride ($ClNO_2$) is a night time radical reservoir that generates chlorine radicals ($Cl^{\cdot}$) upon sunrise (R1, lifetime of $ClNO_2$ (τ_{ClNO2}) $\approx$ 30 min at midday). It is produced through heterogeneous reaction of chloride (Cl^-) containing aerosols and dinitrogen pentoxide (N_2O_5(g)) generated from the reaction between the gas-phase nitrate radical ($NO_3^{\cdot}$) and nitrogen dioxide (NO_2) (R 2-4, (Finlayson-Pitts et al., 1989)). In acidic aerosols (< pH 2) uptake of N_2O_5 (g) can also produce gas-phase chlorine (Cl_2(g), R5), resulting from an enhanced $ClNO_2$ uptake coefficient of up to 3 orders of magnitude (Roberts et al., 2008). During the day, N_2O_5 exists at low levels due to the short lifetime of NO_3 ($\tau_{NO3} < 5$ s) from photolysis and reaction with NO (Wayne et al., 1991). Reactive chlorine can come from both natural sources like sea salt and biomass burning (Blanchard, 1985; Woodcock, 1953), and anthropogenic sources like steel making, incineration, bleaching processes, and coal power plants (Hov, 1985; Reff et al., 2009; Tanaka et al., 2000; Lee et al., 2018). The efficiency of $ClNO_2$ production depends on heterogeneous loss of N_2O_5, which is a function of the N_2O_5 uptake coefficient on aerosols (γ_{N2O5}) and aerosol surface area, and the yield of $ClNO_2$ (Φ_{ClNO2}) (Thornton et al., 2003; Schweitzer et al., 1998; Behnke et al., 1997; Hu and Abbatt, 1997; Bertram and Thornton, 2009). In a nocturnal boundary layer, $ClNO_2$ can accumulate to significant levels due to its long lifetime ($\tau_{ClNO2} > 30$ h) with slow loss mechanisms through heterogeneous uptake (Behnke et al., 1997; Frenzel et al., 1998; George et al., 1995). At sunrise, $ClNO_2$ rapidly photolyzes to generate chlorine radicals ($Cl^{\cdot}$), which can react with most volatile organic compounds (VOCs). For alkanes, $Cl^{\cdot}$ has up to 1 - 2 orders of magnitude larger rate constants than hydroxyl radicals (e.g., $k_{OH+n-C4H10}$ = 2.4 $\times$ 10^{-12}, $k_{Cl+n-C4H10}$ = 2.2 $\times$ 10^{-10} at 298 K) (Atkinson, 1997; Atkinson and Arey, 2003). Therefore, $Cl^{\cdot}$ can potentially influence the radical pool (HO_x-RO_x) and level of ozone (O_3), which can also affect the formation of secondary aerosols. This influence can be most prominent in the morning when concentrations of other oxidants are low (i.e., $NO_3^{\cdot}$ and $^{\cdot}OH$) (Finlayson-Pitts, 1993; Hov, 1985; Young et al., 2014).

Atmos. Chem. Phys. Discuss., https://doi.org/10.5194/acp-2018-1216
Manuscript under review for journal Atmos. Chem. Phys.
Discussion started: 27 November 2018

Atmospheric Chemistry and Physics Discussions

$$ClNO_{2(g)} + h\nu \rightarrow Cl^{\cdot}_{(g)} + NO_{2(g)} \quad \text{(R1)}$$

$$NO_{2(g)} + O_{3(g)} \rightarrow NO^{\cdot}_{3(g)} + O_{2(g)} \quad \text{(R2)}$$

$$NO^{\cdot}_{3(g)} + NO_{2(g)} \rightleftharpoons N_2O_{5(g)} \quad \text{(R3)}$$

$$N_2O_{5(g)} + Cl^{-}_{(aq)} \rightarrow ClNO_{2(g)} \quad \text{(R4)}$$

$$ClNO_{2(g)} + Cl^{-}_{(aq)} + H^{+}_{(aq)} \rightarrow Cl_{2(g)} + HNO_{2(aq)} \quad \text{(R5)}$$

The first ambient measurement of $ClNO_2$ was carried out by Osthoff et al. (2008) at the coast of southeastern U.S. In that study, $ClNO_2$ was observed up to ~1 ppb at night time, influenced by urban air and ship plumes. Since then, a growing number of measurements reported significant levels of $ClNO_2$, especially in polluted, coastal regions with sources from natural and anthropogenic chloride and nitrogen oxides. Riedel et al. (2012) measured up to ~2 ppb of $ClNO_2$ on board a research vessel (Atlantis) during the CalNex 2010 field campaign, and the maximum level was observed in Santa Monica Bay downwind of Los Angeles. Recent studies show that high levels of $ClNO_2$ are also present in mid-continental regions. Thornton et al. (2010) measured up to ~ 400 ppt in Boulder, Colorado, which is ~ 1,400 km away from the coastline. Mielke et al. (2011) reported up to ~ 250 ppt in Calgary, Alberta, Canada, during spring, which is ~ 800 km from the coastline. Back trajectory analysis results showed that the observations were most likely not influenced by marine airmasses. Overall, observations have shown that $ClNO_2$ is ubiquitous in the troposphere.

However, measurements are still limited, with discrepancies remaining between model and measurements. Modeling studies have consistently suggested the significance of $Cl^{\cdot}$ initiated reactions in regional and global O_3 production and in the lifetime of trace gases (e.g., VOCs, mercury, etc.) in the troposphere (Knipping and Dabdub, 2003; Tanaka et al., 2000, 2003; Sarwar et al., 2014; Sherwen et al., 2016; Simon et al., 2009). Sarwar et al. (2014) explored the production of $ClNO_2$ from sea salt and biomass burning and its impact in the Northern Hemisphere by including $ClNO_2$ formation chemistry in the Community Multiscale Air Quality (CMAQ v 5.0.2) model. The results showed that, compared to the simulations without $ClNO_2$ formation, monthly 8 h wintertime maximum O_3 and ·OH increased up to 7 ppb and 20 % respectively. The production and its subsequent influence was the largest in China and Western Europe. In the Hong Kong-Pearl River Delta (HK-PRD) region, Li et al. (2016) simulated up to ~ 1 ppb of $ClNO_2$ originating from sea salt, biomass burning, and anthropogenic emissions (e.g., coal combustion) with the Weather Research and Forecasting coupled with Chemistry (WRF-CHEM) model. This resulted in ~16 % O_3 increase in the planetary boundary. The assessments using global chemical transport models are likely lower end estimates since they tend to underestimate $ClNO_2$ due to limited emission inventories. Moreover, low resolution of the grid can also lead to an underestimation of $ClNO_2$ due to smoothing out local $ClNO_2$ peaks and also by diluting local NO_x emissions, that will result in limited NO_3 and N_2O_5 production. According to Sarwar et al. (2012, 2014), the CMAQ model with a finer grid (i.e. 12 km) simulated $ClNO_2$ that corresponded better to the observations, compared to the models runs with coarser grid size (i.e., 108 km), embedded with similar chemistry. Another modeling study by Sherwen et al. (2017) compared the $ClNO_2$ levels between the GEOS-Chem simulations and observations in inland areas (i.e., London, UK and a mountain top

Atmos. Chem. Phys. Discuss., https://doi.org/10.5194/acp-2018-1216
Manuscript under review for journal Atmos. Chem. Phys.
Discussion started: 27 November 2018

Atmospheric Chemistry and Physics Discussions

near Frankfurt, Germany) during the summer of 2015. Compared to observations, the simulations underestimated the $ClNO_2$ maxima levels by $\sim$ 7 times in inland areas.

Although only a small number of observations in Asia have been conducted in comparison to North America/Europe, previous studies in Asia have consistently shown significant levels of $ClNO_2$ present in the troposphere (Liu et al., 2017; Tham et al., 2016; Wang et al., 2016, 2017). $ClNO_2$ observations at semi-rural (Wangdu of Hebei province) and urban (Hong Kong, Jinan) regions in China have measured up to 2 ppb and 776 ppt respectively. At the mountain top (957 m above sea level) in Hong Kong, up to 4.7 ppb of $ClNO_2$ was reported. The high levels of $ClNO_2$ in these studies were mostly correlated to continental pollution from sources nearby (e.g., power plant plumes, biomass burning). East Asian countries are of particular interest due to the rapid economic growth in the past decades with high anthropogenic emissions from densely populated megacities (e.g., Shanghai, Guangzhou, Beijing, Tokyo, Seoul). The majority of the world's mega-cities are situated in coastal regions (Neumann et al., 2015) with high NO_x emissions and abundant sources of chloride from both anthropogenic and natural origin. These regional characteristics likely promote $ClNO_2$ production. Moreover, considering that nearly half the population in the world lives near the coast (defined as $<$ 100km from coastline, (Hinrichsen, 1998)), a careful evaluation of the impact of $ClNO_2$ on local tropospheric chemistry is crucial.

In this study, we present $ClNO_2$ observation results during the Korean - United States Air Quality (KORUS-AQ) study conducted in the Seoul Metropolitan Area (SMA), South Korea during late Spring (May 2 to June 12, 2016). The field campaign was an international collaboration between the National Aeronautics and Space Administration (NASA) of the United States and the National Institute of Environmental Research (NIER) of South Korea with the aim to better understand the impact of mega-cities on regional air quality. A comprehensive suite of measurements were conducted at two super sites (Olympic Park site, OP; Taewha Research Forest, TRF), and included airborne observations, that were conducted aboard the NASA DC-8 over the South Korean peninsula and the Yellow Sea. By combining airborne and ground measurements from the urban center (OP) and a forested region downwind (TRF), we investigate possible influences of $ClNO_2$ on tropospheric air quality in SMA.

2 Methods

2.1 KORUS-AQ 2016 Field Campaign and Observation Sites

We present observations carried out at Olympic Park, (OP; lat:37° 30' 32.904" N, lon:127° 7' 20.136" E) and Taehwa Research Forest (TRF; lat: 37° 19' 14.484" N, lon:127° 18' 32.58" E) and on the NASA DC-8 airborne laboratory. The two ground sites were within the SMA region, which is the second largest metropolitan area in the world with a population of $\sim$ 25.6 million people. As shown in Figure 1(a), the OP site is located in the southern part of Seoul, surrounded by high rise residence buildings and close to major freeways. The TRF site is in the middle of a forested area, $\sim$ 26 km southeast of the OP site. Previous studies have shown that the TRF site has complex chemistry, affected by both aged anthropogenic air masses from the city and fresh biogenic emissions from the forest (Kim et al., 2016, 2015). Both sites were $\sim$ 50 km to the east of the nearest coastline. Figure 1(b) shows the tracks of the research flights during the whole campaign when $ClNO_2$ was measured. Spiral patterns were conducted near the TRF site to measure a vertical profile of the troposphere. Airborne observations were carried out during the

Atmos. Chem. Phys. Discuss., https://doi.org/10.5194/acp-2018-1216
Manuscript under review for journal Atmos. Chem. Phys.
Discussion started: 27 November 2018

Atmospheric Chemistry and Physics Discussions

daytime, between 8:00 and 17:00 local time. A summary of the analytical techniques of the measurements presented in this study are shown in Table 1.

2.2 Chemical Ionization Mass Spectrometry and Calibration

A THS Instruments LLC Chemical Ionization Mass Spectrometer (CIMS), using iodide (I^-) as the reagent ion was used for measuring Cl_2 and $ClNO_2$. The system was similar to what is described in Slusher et al. (2004) and Liao et al. (2011), and the inlet configuration during the campaign is shown in Figure S1. Ambient air was sampled through a stainless steel donut shaped inlet at TRF and a PTFE tube inlet at OP. The stainless steel donut inlet has been shown to effectively avoid wall loss of reactive halogens during previous campaigns (Liao et al., 2011). However, artifacts of $ClNO_2$ of Cl_2 from interactions on the inlet has been shown to be negligible in field conditions (Riedel et al., 2012; Thornton et al., 2010; Liao et al., 2014). Therefore, the use of different types of inlets in the two ground sites and on the DC-8 is not expected to be an issue for the quantitative comparisons in this study. The sampled air went through the first 3-way valves to be delivered to an ambient or charcoal scrubber mode for background, alternating every 5 minutes. The second 3-way valve was for heated (150 ^{o}C) and unheated cycles, and $ClNO_2$ and Cl_2 were only quantified during the unheated cycles to avoid any potential artifacts, as described in Liu et al. (2017). Additional flow of 4 slpm was drawn at the end of the inlet to reduce the residence time and 1 slpm was sampled into the CIMS. All the inlet parts, after the blower, including the fittings and tubings, were made of Polytetrafluoroethylene (PTFE). In the flow tube, the target compounds form clusters with I^- (R 5-6, (Huey, 2007; Huey et al., 1995; McNeill et al., 2006)), which were generated by flowing 1 slpm N_2 through a methyliodide (CH_3I) permtube oven maintained at 50 ^{o}C . Polonium (NRD LLC, Static Master, Model: 2U500, Activity: 20 mCi) was used as the radioactive source for ionization. Clusters of Cl_2 isotopes were detected at the mass to charge ratio *(m/z)* of 197 and 199, and $ClNO_2$ was measured at 208 and 210. The natural abundance of Cl_2 and $ClNO_2$ isotopes are approximately 9:6:1 ($^{35}Cl^{35}Cl$: $^{35}Cl^{37}Cl$: $^{37}Cl^{37}Cl$) and 3:1 ($^{35}ClNO_2$: $^{37}ClNO_2$) respectively.

$$ClNO_{2(g)} + I^- \rightarrow IClNO_2^-{}_{(g)} \quad \text{(R6)}$$

$$Cl_{2(g)} + I^- \rightarrow ICl_2^-{}_{(g)} \quad \text{(R7)}$$

Calibrations of Cl_2 and $ClNO_2$ were carried out during and after the campaign. Cl_2 in a cylinder (Airgas, 10 ppm in N_2) was diluted with zero air to be sampled in either ambient or scrubber (charcoal) mode (Figure S1). The Cl_2 in the cylinder was quantified through the method described by Liao et al. (2012) and was 8.84 $\pm$ 0.43 ppm. $ClNO_2$ was synthesized, based on Thaler et al. (2011). Briefly, Cl_2 gas in N_2 was passed through a pyrex reservoir (diameter = 1.3 cm, length = 5.5 cm) containing a bed of NaCl (MACRON) and $NaNO_2$ (Sigma Aldrich) with a molar ratio of 10 to 1. This slurry mixture contains NO_2^- that will react with the flowing Cl_2 and generate $ClNO_2$. The output flow was further diluted with 4 L min^{-1} of zero air in order to sufficiently provide gas flow. The flow containing synthesized $ClNO_2$ was then analyzed at *m/z* of 208 and 210 with the CIMS. NO_2 and NO-NO_y were simultaneously measured with a Cavity Ring Down Spectroscopy (CRDS, Los Gatos Research, detection limit: 10 ppt, precision: 50 ppt at 1σ, model: 907-0009-0002) and chemiluminescence (CL, Thermo

Atmos. Chem. Phys. Discuss., https://doi.org/10.5194/acp-2018-1216
Manuscript under review for journal Atmos. Chem. Phys.
Discussion started: 27 November 2018

Scientific, detection limit: 50 ppt, model: 42 i) respectively. $ClNO_2$ is detected as NO_y in the CL through conversion to NO on the heated (325 ^{o}C) molybdenum converter. Therefore, $ClNO_2$ could be determined by comparing the three instruments and subtracting the byproducts (HONO and NO_2) from the total NO_y.

2.3 Modeling

We used Framework for 0-D Atmospheric Modeling (F0AM v3.1) for simulating $ClNO_2$ production and testing the impact of measured $ClNO_2$ on the regional tropospheric chemistry (e.g., O_3 production). F0AM is a MATLAB based open-source box model. Detailed descriptions of the model can be found in Wolfe et al. (2016). The model was constrained with meteorology parameters and trace gases observed during the campaign. The constrained trace gases include CO, NO, CH_4, and 20 non-methane hydrocarbons including 8 alkanes (i.e., ethane, propane, iso-butane, n-butane, iso-pentane, n-pentane, n-hexane, and n-heptane), that have relatively high reaction rate constants with Cl·. For photolysis rate constants, the hybrid method (Wolfe et al., 2016) was used and scaled to the rates calculated from the actinic flux measured on-board the DC-8 (< 1km). The Master Chemical Mechanism v3.3.1 (MCM) was embedded in the model from http://mcm.leeds.ac.uk/MCM, with a detailed gas photochemistry (i.e., 5832 species and 17224 reactions), including the oxidation of CH_4 and 142 non-methane primary emitted VOCs (Jenkin et al., 2015). Since MCM v3.3.1 only includes $Cl^·$ reactions with alkane species, we embedded additional $Cl^·$ chemistry in the model, similar to what Riedel et al. (2014) reported, by including multiple $Cl^·$ precursors (e.g., Cl_2, $ClNO_2$, HCl, $ClONO_2$, HOCl) and $Cl^·$ reactions with non-alkane VOCs, such as alkene, alcohol, aromatics, alkynes, ketones, organic acids and nitrates. For simulating $ClNO_2$ production, the model was constrained with airborne observations during the campaign. γ_{N2O5} was calculated from the Bertram and Thornton (2009) study with water content derived from the thermodynamic model Extended Aerosol Inorganics Model (E-AIMS, (Clegg et al., 1998; Friese and Ebel, 2010)), and the measured inorganic aerosol compostion, temperature, and relative humidity. Discussion on how E-AIM was modeled is presented in the supplement. The average and median γ_{N2O5} value during the whole campaign were both 0.017. Aerosol surface area was calculated from the measured particle size distributions for particle sizes between 10 nm and 5 μm. The FLEXible PARTicle dispersion model (FLEXPART v9.1, https://www.flexpart.eu) was used for the airmass source contribution and backward trajectory analysis.

3 Results and Discussions

3.1 $ClNO_2$ Observations

Figure 2 shows the temporal variation of trace gases measured during the campaign at (a) the OP site (May 17th - June 11th) and (b) the TRF site (May 5th - June 11th). The OP site, which was located near heavy traffic, showed high levels of NO_x and O_3 throughout the campaign. In most of the nights (except for May 24th - 26th, 30th - 31st, and June 6th - 7th), O_3 was titrated by NO. On the other hand, at the TRF site, which is a forested region downwind of the urban area, O_3 remained at $\sim$ 30 ppb throughout the night. During the measurement period, measureable amounts of $ClNO_2$ were observed at both ground

Atmos. Chem. Phys. Discuss., https://doi.org/10.5194/acp-2018-1216
Manuscript under review for journal Atmos. Chem. Phys.
Discussion started: 27 November 2018

sites (Figure 3). The maximum observed $ClNO_2$ was ~800 ppt (10 min averaged) and ~2.5 ppb (5 min averaged) at the OP and TRF sites, respectively. In both sites, $ClNO_2$ started accumulating at sunset and rapidly photolyzed upon sunrise, which was ~5:30 local standard time (LST) during the campaign.

Daytime (11:00 - 18:00, LST) $ClNO_2$ was up to ~100 ppt at OP and ~250 ppt at TRF (Figure 4). The level showed a positive correlation to Cl_2, especially in relatively high O_3 conditions (> 50 ppb). When O_3 was relatively low, Cl_2 production was suppressed, while $ClNO_2$ was not necessarily limited. Excluding the days with low O_3 (i.e., May 26th and 29th for OP and May 6th, 29th, and June 4th for TRF), the relationship between daytime $ClNO_2$ and Cl_2 showed moderate to high correlations with R^2 of 0.49 and 0.80 for OP and TRF, respectively. This positive correlation is very similar to the results reported by Liu et al. (2017) from the North China Plain in June 2014. In their study, up to ~ 450 ppt of both Cl_2 and $ClNO_2$ was measured during the daytime (10:00 - 20:00, LST), with strong correlation of R^2 = 0.83. Cl_2 levels were also suppressed in low O_3 and OH conditions during low solar radiation periods. Therefore, the authors suggested that daytime Cl_2 levels could be affected by photochemical reactions (or products). Considering the short lifetime of Cl_2 and $ClNO_2$ during the day (i.e., 11:00 - 18:00 LST in our study), the levels we observed are likely affected through local production. According to Liu et al. (2017), the airmass showed moderate correlation to SO_2 with possible influences from power plants. However, in our study, the $ClNO_2$ measured at both the OP and TRF site weakly correlated with SO_2 (R^2 = 0.02). Previous studies have shown that N_2O_5 uptake efficiency on aerosols could be affected by organic content of particles (McDuffie et al., 2018; Thornton et al., 2003). However, we weren't able to identify a correlation. Rather, there is a possibility that the positive correlation of Cl_2 and $ClNO_2$ could be coming from reactions in acidic particles. $ClNO_2$, generated from N_2O_5 partitioning on Cl^- containing aerosols, is very insoluble (γ_{ClNO2} $\approx 10^{-6}$, (Rossi, 2003)) in near-neutral pH, and therefore readily partition into gas-phase. However, according to Roberts et al. (2008), in acidic media (< pH 2), $ClNO_2$ has higher uptake coefficients (up to 3 orders of magnitude), which can lead to direct production of Cl_2. Indeed, aerosol acidity was mostly below pH 2 during the campaign, based on thermodynamic calculations, constrained with airborne observations (Figure S3). Therefore, further investigation is required on the roles of aerosols acidity on the generation of gas-phase Cl_2 and $ClNO_2$.

3.2 Sources of $ClNO_2$

FLEXPART source contribution analysis shows that the level of $ClNO_2$ at the ground sites highly correlated to the origin of the air mass (Figure 3). During the nights in red shade (OP: May 20th, 22nd, June 2nd, and 7th; TRF: May 11th, 19th-22nd, June 2nd, and June 6th-7th), there was limited production of $ClNO_2$. This period corresponded to low contribution of airmasses originating from the ocean and limited particle chloride measured by the aerosol mass spectrometer (AMS) at the ground site for OP and airborne over TRF. Whether the chloride is from the ocean or anthropogenic emissions is unclear since large point sources (such as power plants or petrochemical facilities) are also present along the west coast of the SMA. At OP, when nitrate production was limited due to O_3 titration, $ClNO_2$ was negligible even with the presence of chloride. On the nights of May 20th and May 22nd, rapid changes in air quality were observed with fast shifts in O_3, SO_2, and CO, which also corresponded with changes in $ClNO_2$ and Cl_2 (Figure S4). These events suggest the importance of boundary layer advection in controlling the $ClNO_2$ levels in the region.

Atmos. Chem. Phys. Discuss., https://doi.org/10.5194/acp-2018-1216
Manuscript under review for journal Atmos. Chem. Phys.
Discussion started: 27 November 2018

Atmospheric Chemistry and Physics Discussions

The two ground sites showed rather different diurnal variations, affected by their chemical regimes. Figure 5 shows diurnal averages of $ClNO_2$ and other trace gases. Two different diurnal trends of $ClNO_2$ between OP and TRF were observed. The measurements were averaged over selected days (OP: May 18th-20th, 22nd, 23rd, 29th, June 4th; TRF: May 5th, 8th, 9th, 12th, 17th, 18th, 30th, June 8th, 10th) that showed these two distinct profiles at each site, which we will further discuss. At the TRF site, far from direct NO emissions, significant levels of $ClNO_2$ was sustained throughout the night in most of the observation period with rapid photolysis upon sunrise. On the other hand, at OP (Figure 5 (a)), $ClNO_2$ started to increase upon sunset, followed by a rapid drop at around 22:00 LST. The trend was consistent with slow nitrate radical production rate, calculated from measured NO_2 and O_3 at the site. The wind direction, SO_2, and CO did not correlate. The boundary layer at night becomes shallower (200 - 300 m) compared to during the day (1-2 km). The diurnal variations at OP show that NO levels were sustained high in this shallow nocturnal boundary layer throughout the night and often titrated O_3 to zero. Suppressed $ClNO_2$ production resulting from NO_3 and O_3 titration by NO has been observed in urbanized regions near surfaces (Osthoff et al., 2014), which is the case of the OP site close to NO emission sources. However, significant levels of N_2O_5 and $ClNO_2$ could have been present in the upper part of the surface layer. During the 2015 Megacity Air Pollution Study (MAPS, Seoul, 2015), a Cavity Enhanced Spectroscopy (CES) instrument was installed on top of the Seoul tower in the May - June period for N_2O_5 measurements (Brown et al., 2017). The elevation of the measurement site was 360 m above sea level (ASL), allowing for sampling further away from direct NO emissions. In their study, the average nighttime O_3 was around 50 ppb and N_2O_5 was observed in most of the nights, reaching up to 5 ppb. Therefore, it is reasonable to speculate that $ClNO_2$ could have been present in higher levels than reported in this study. It is very likely that $ClNO_2$ levels higher than the surface measurements could have been present at higher elevation during the observation period.

At both sites, elevated levels of $ClNO_2$ were present 4-5 hours after sunrise. $ClNO_2$, in the morning, positively correlated to Cl_2 levels, but $ClNO_2$ did not follow the nitrate production rate at the site (Figure S5). A box model run, initially constrained with observed $ClNO_2$ at sunrise, simulated rapid photolysis that corresponded to the observation until 7 am LST (Figure S6). However, between 7 and 8 am LST, a second $ClNO_2$ peak was observed at TRF (Figure 5 (b)), a trend that was observed about half the observation days. With the net $ClNO_2$ production rate from the observation, and the loss rate from the simulated $ClNO_2$ from photolysis, a production rate of 400 ppt h^{-1} would be required to reconcile the observation. In the case of $ClNO_2$ observed on May 5th at TRF, a maximum of 2.5 ppb h^{-1} of $ClNO_2$ production rate was required in the morning to reconcile the observations (An insert of Figure S6 (b)). In the case of OP, 18 ppt h^{-1} would be required for the 7 averaged days. The $ClNO_2$ production rate required in the morning at TRF was much higher than the previous studies that have also reported high sustained levels of $ClNO_2$ in the morning (i.e., 20 - 200 ppt h^{-1}) (Faxon et al., 2015; Bannan et al., 2015; Tham et al., 2016). In these previous studies, three possibilities have been suggested that could explain the high sustained levels of $ClNO_2$ in the early morning : 1) entrainment of $ClNO_2$ from residual layer, 2) in-situ generation of $ClNO_2$, and 3) transport of $ClNO_2$ within the boundary layer. Each possibility is explored below.

In the night time, the nocturnal boundary layer is decoupled from the residual layer (Stull, 1988), where the pollution from the previous day resides. Being removed from direct NO emissions near the surface, N_2O_5 can effectively accumulate in the residual layer, with the major loss process being heterogeneous reaction on aerosols. Therefore, high levels of NO_2 and O_3

Atmos. Chem. Phys. Discuss., https://doi.org/10.5194/acp-2018-1216
Manuscript under review for journal Atmos. Chem. Phys.
Discussion started: 27 November 2018

Atmospheric Chemistry and Physics Discussions

formed during the day can be trapped in the residual layer and result in significant levels of $ClNO_2$ persisting throughout the night. Figure 6, shows (a) regional and (b) vertical distribution of airborne $ClNO_2$ throughout the campaign in the morning (8:00 - 8:30 LST) over the SMA region (lat: 37^o 12' 0" N - 37^o 38' 60" N, lon: 126^o 54' 0" E - 127^o 47' 60" E). During 3 flights (i.e., May 25th, May 31st, and June 10th), $ClNO_2$ was observed in the residual layer with a max of $\sim$ 230 ppt. However in rest of the flights, an average of only 17 $\pm$ 56 ppt of $ClNO_2$ (black circles) was observed. Even the three days (i.e., May 25th, 31st, and June 10th), that $ClNO_2$ was observed in the residual layer, the level (max 230 ppt) could not reconcile the observed levels at the TRF site, which was 342 $\pm$ 330 ppt when averaged over the corresponding 3 days at 8:00 - 8:30 LST.

In order to further explore the possibility of in-situ formation, box model simulations of $ClNO_2$ production from heterogeneous reaction of N_2O_5 and chloride containing aerosols were conducted. N_2O_5 was calculated assuming a photo-stationary state of NO_3 (Brown et al., 2005) and aerosol surface area was taken from airborne observations over TRF. Based on the box model results in Figure 9, even with an assumption of 100 % yield, $ClNO_2$ from heterogeneous reaction was not able to reconcile the observed level. The box model analysis was carried out to also explore the possibility of gas phase production (i.e., $Cl\cdot_{(g)} + NO_{2(g)} + M \rightarrow ClONO_{(g)} + M$, $Cl\cdot_{(g)} + NO_{2(g)} + M \rightarrow ClNO_{2(g)} + M$) of $ClNO_2$ (Figure S8). The simulations show that only 2-10 ppt of $ClNO_2$ and ClONO can be produced during the day.

Therefore, the third possibility, local transport within the boundary layer, would be the most likely explanation for the high $ClNO_2$ in the morning based on our analysis. Although $ClNO_2$ readily photolyzes during the day ($\tau_{ClNO2} \approx$ 30 min at midday), the lifetime could be significantly long enough in the early morning to allow for transport of $ClNO_2$ to the ground sites. Based on the NCAR Tropospheric Ultraviolet and Visible (TUV v5.2) model, the lifetime of $ClNO_2$, averaged between 5:30 and 8:30 LST was $\sim$ 2 hours during the campaign, under clear sky conditions. Figure 8 shows back trajectory analysis initiated at 9 am local time at TRF. At high $ClNO_2$ days with the morning peaks, most of the air masses originiated from the west. In the west, there could have been favorable conditions for $ClNO_2$ to build up, such as high chloride content in aerosols from both anthropogenic and natural sources and high levels of NO_x-O_3 to generate N_2O_5 at night. Therefore, significant levels of $ClNO_2$ produced during the night in the west could have been transported to TRF before being completely photolyzed.

3.3 Impacts of $ClNO_2$ on O_3

Cl· produced from $ClNO_2$ photolysis can influence the local air quality through reactions with VOCs followed by enhanced production of O_3. In order to investigate the possible impact of Cl· initiated reactions on the local chemistry, we carried out a box model analysis constrained with observations of $ClNO_2$, NO and VOCs described in the method. The diurnal variation of $ClNO_2$ constrained in the box model was averaged for the same days shown in Figure 5. The results show that when the model was constrained with $ClNO_2$ and Cl· initiated chemistry, higher levels of O_3 were simulated (Figure 9). The averaged net O_3 production rate was enhanced by up to 2 % and 25 % at OP and TRF in the morning and by 1 % and 2 % when averaged during the day. Although the OP site has higher alkane levels than the TRF site, Cl· in the morning were around 7 times lower due to the low $ClNO_2$ levels ($\sim$60 ppt) in the morning. For OH, the net production rate at TRF increased by 2 % in the morning. The results particularly from TRF are comparable with the previous study in the mountaintop site in Hong Kong, China (Wang

et al., 2016). The enhancement of ozone (max - min) was higher than their moderate $ClNO_2$ case (11 %) but lower than the high $ClNO_2$ plume case (41 %).

4 Conclusions

A comprehensive suite of measurements of $ClNO_2$, other trace gases, and aerosol concentrations and properties have been conducted on the DC-8 and at two ground sites during the KORUS-AQ 2016 field campaign. The observed averaged diurnal variations are consistent with the previous observations and our understanding on the photochemistry of $ClNO_2$. In addition, the presence of $ClNO_2$ was substantially suppressed during strong stagnation events, which could have prevented the transport of chloride from the coast. High levels of $ClNO_2$ were sustained for 4-5 hours after sunrise, which requires significant production of $ClNO_2$ (up to 2.5 ppb h^{-1}). We did not find any empirical evidence to support the hypothesis raised by previous studies, where they attributed high sustained $ClNO_2$ in the morning to transport from the residual layer Tham et al. (2016); Wang et al. (2016). Moreover, box model simulations of heterogeneous and gas-phase reactions only generated about 10 ppt of $ClNO_2$, and thus could not reconcile the discrepancies. Rather, local transport of $ClNO_2$ from highly polluted airmasses, originating from the west, is the most likely explanation. Finally, box model simulations constrained with observations suggest that Cl· initiated chemistry can lead up to ∼25 % increase of net O_3 production rate in the morning.

Data availability. Dataset used in this study is open to public and can be downloaded at https://www-air.larc.nasa.gov/missions/korus-aq/

Author contributions. DJ, RS, DG, YL, DT, SK, and GH designed and executed field measurements for collecting $ClNO_2$ and Cl_2; BAN, JLJ, and PCJ provided the airborne AMS data; CK ran the FLEXPART analysis; TM and JS provided O_3 measurements; DRB provided the WAS data; DS and AG provided the PTR-ToF-MS data; RL provided NO_x and O_3 data; BA provided the data from LARGE; SRH and KU provided data from CAFS; HS provided AMS data at OP; SH provided HCHO measurements at TRF; YL, DK, and JA provided CO measurements at TRF. DJ and SK prepared the original manuscript, and all other authors contributed in editing the manuscript.

Acknowledgements. This study is supported by NASA (NNX15AT90G) and NIER. CU HR-AMS measurements and pH and aerosol liquid water calculations (BAN, PCJ, and JLJ) were supported by NASA grant NNX15AT96G and 80NSSC18K0630. We thank the Wisthaler research group (University of Oslo, University of Innsbruck) for providing airborne VOC data, John Crounse and Paul Wennberg(CALTECH) for the HNO_3 data, and Hwajin Kim (Korea Institute of Science and Technology) for the discussions on aerosol composition. The authors appreciate logistical support from the research and supporting staff at Taehwa research forest operated by Seoul National University.

Atmos. Chem. Phys. Discuss., https://doi.org/10.5194/acp-2018-1216
Manuscript under review for journal Atmos. Chem. Phys.
Discussion started: 27 November 2018

Atmospheric Chemistry and Physics Discussions

References

Atkinson, R.: Gas-Phase Tropospheric Chemistry of Volatile Organic Compounds: 1. Alkanes and Alkenes, J. Phys.Chem. Ref. Data, 26, 215–290, https://doi.org/10.1063/1.556012, 1997.

Atkinson, R. and Arey, J.: Gas-phase tropospheric chemistry of biogenic volatile organic compounds: A review, Atmos. Environ., 37, S197–S219, https://doi.org/https://doi.org/10.1016/S1352-2310(03)00391-1, 2003.

Bannan, T. J., Booth, A. M., Bacak, A., Muller, J. B. A., Leather, K. E., Breton, M. L., Jones, B., Young, D., Coe, H., Allan, J., Visser, S., Slowik, J. G., Furger, M., Prévôt, A. S. H., Lee, J., Dunmore, R. E., Hopkins, J. R., Hamilton, J. F., Lewis, A. C., Whalley, L. K., Sharp, T., Stone, D., Heard, D. E., Fleming, Z. L., Leigh, R., Shallcross, D. E., and Percival, C. J.: The first UK measurements of nitryl chloride using a chemical ionization mass spectrometer in central London in the summer of 2012, and an investigation of the role of Cl atom oxidation, J. Geophys. Res. Atmos., 120, 5638–5657, https://doi.org/10.1002/2014JD022629, 2015.

Behnke, W., George, C., Scheer, V., and Zetzsch, C.: Production and decay of $ClNO_2$ from the reaction of gaseous N_2O_5 with NaCl solution: Bulk and aerosol experiments, J. Geophys. Res. Atmos., 102, 3795–3804, https://doi.org/10.1029/96JD03057, 1997.

Bertram, T. H. and Thornton, J. A.: Toward a general parameterization of N_2O_5 reactivity on aqueous particles: the competing effects of particle liquid water, nitrate and chloride, Atmos. Chem. Phy., 9, 8351–8363, https://doi.org/10.5194/acp-9-8351-2009, 2009.

Blanchard, D.: The oceanic production of atmospheric sea salt, J. Geophys. Res., 90, 961–963, http://onlinelibrary.wiley.com/doi/10.1029/JC090iC01p00961/full, 1985.

Brown, S. S., Osthoff, H. D., Stark, H., Dubé, W. P., Ryerson, T. B., Warneke, C., de Gouw, J. A., Wollny, A. G., Parrish, D. D., Fehsenfeld, F. C., and Ravishankara, A. R.: Aircraft observations of daytime NO_3 and N_2O_5 and their implications for tropospheric chemistry, J. Photochem. Photobiol. A Chem., 176, 270–278, https://doi.org/10.1016/j.jphotochem.2005.10.004, 2005.

Brown, S. S., An, H. J., Lee, M., Park, J. H., Lee, S. D., Fibiger, D. L., McDuffie, E. E., Dubé, W. P., Wagner, N. L., and Min, K. E.: Cavity enhanced spectroscopy for measurement of nitrogen oxides in the Anthropocene: results from the Seoul tower during MAPS 2015, Faraday Dicuss., 200, 529–557, https://doi.org/10.1039/C7FD00001D, 2017.

Clegg, S. L., Brimblecombe, P., and Wexler, A. S.: Thermodynamic Model of the System $H^+ - NH_4^+ - SO_4^{2-} - NO_3^- - H_2O$ at Tropospheric Temperatures, J. Phys. Chem. A, 102, 2137–2154, https://doi.org/10.1021/jp973042r, http://pubs.acs.org/doi/abs/10.1021/jp973042r, 1998.

Colman, J. J., Swanson, A. L., Meinardi, S., Sive, B. C., Blake, D. R., and Rowland, F. S.: Description of the analysis of a wide range of volatile organic compounds in whole air samples collected during PEM-Tropics A and B, Anal. Chem., 73, 3723–3731, https://doi.org/10.1021/ac010027g, 2001.

Faxon, C., Bean, J., and Ruiz, L.: Inland Concentrations of Cl_2 and $ClNO_2$ in Southeast Texas Suggest Chlorine Chemistry Significantly Contributes to Atmospheric Reactivity, Atmosphere, 6, 1487–1506, https://doi.org/10.3390/atmos6101487, 2015.

Finlayson-Pitts, B. J.: Chlorine Atoms as a Potential Tropospheric Oxidant in the Marine Boundary Layer, Res. Chem. Intermediat., 19, 235–249, https://doi.org/10.1163/156856793X00091, 1993.

Finlayson-Pitts, B. J., Ezell, M. J., and Pitts Jr, J. N.: Formation of chemically active chlorine compounds by reactions of atmospheric NaCl particles with gaseous N_2O_5 and $ClONO_2$, Nature, 337, 241–244, https://doi.org/https://doi.org/10.1038/337241a0, 1989.

Frenzel, A., Scheer, V., Sikorski, R., George, C., Behnke, W., and Zetzsch, C.: Heterogeneous Interconversion Reactions of $BrNO_2$, $ClNO_2$, BrO_2, and ClO_2, J. Phys. Chem. A, 102, 1329–1337, https://doi.org/10.1021/jp973044b, http://dx.doi.org/10.1021/jp973044b, 1998.

Friese, E. and Ebel, A.: Temperature Dependent Thermodynamic Model of the System $H^+-NH_4^+-Na^+-SO_4^{2-}-NO_3^--Cl^--H_2O$, J. Phys. Chem. A, 114, 11 595–11 631, https://doi.org/10.1021/jp101041j, 2010.

George, C., Behnke, W., Scheer, V., Zetzsch, C., Magi, L., Ponche, J. L., and Mirabel, P.: Fate of $ClNO_2$ over aqueous solutions containing iodide, Geophys. Res. Lett., 22, 1505–1508, https://doi.org/10.1029/95GL01417, 1995.

Hinrichsen, D.: Costal Waters of the World: Trends, Threats, and Strategies, Island Press, Washington, DC, http://arp.sagepub.com/content/30/4/473, 1998.

Hov, O.: The effect of chlorine on the formation of photochemical oxidants in Southern Telemark, Norway, Atmos. Environ., 19, 471–485, https://doi.org/10.1016/0004-6981(85)90168-4, 1985.

Hu, J. H. and Abbatt, J. P. D.: Reaction probabilities for N_2O_5 hydrolysis on sulfuric acid and ammonium sulfate aerosols at room temperature, J. Phys. Chem. A, 101, 871–878, https://doi.org/10.1021/jp9627436, 1997.

Huey, L. G.: Measurement of Trace Atmospheric Species by Chemical Ionization Mass Spectrometry: Speciation of Reactive Nitrogen and Future Directions, Mass Spectrom. Rev., 26, 166–184, https://doi.org/10.1002/mas.20118, 2007.

Huey, L. G., Hanson, D. R., and Howard, C. J.: Reactions of SF_6^- and I^- with atmospheric trace gases, J. Geophys. Res., 99, 5001–5008, https://doi.org/10.1021/j100014a021, 1995.

Jenkin, M. E., Young, J. C., and Rickard, A. R.: The MCM v3.3.1 degradation scheme for isoprene, Atmos. Chem. Phy., 15, 11 433–11 459, https://doi.org/10.5194/acp-15-11433-2015, 2015.

Kim, S., Kim, S. Y., Lee, M., Shim, H., Wolfe, G. M., Guenther, A. B., He, A., Hong, Y., and Han, J.: Impact of isoprene and HONO chemistry on ozone and OVOC formation in a semirural South Korean forest, Atmos. Chem. Phy., 15, 4357–4371, https://doi.org/10.5194/acp-15-4357-2015, 2015.

Kim, S., Sanchez, D., Wang, M., Seco, R., Jeong, D., Hughes, S., Barletta, B., Blake, D. R., Jung, J., Kim, D., Lee, G., Lee, M., Ahn, J., Lee, S. D., Cho, G., Sung, M. Y., Lee, Y. H., Kim, D. B., Kim, Y., Woo, J. H., Jo, D., Park, R., Park, J. H., Hong, Y. D., and Hong, J. H.: OH reactivity in urban and suburban regions in Seoul, South Korea-an East Asian megacity in a rapid transition, Faraday Dicuss., 189, 231–251, https://doi.org/10.1039/c5fd00230c, 2016.

Knipping, E. M. and Dabdub, D.: Impact of chlorine emissions from sea-salt aerosol on coastal urban ozone, Environ. Sci. Technol., 37, 275–284, https://doi.org/10.1021/es025793z, 2003.

Lee, B. H., Lopez-Hilfiker, F. D., Schroder, J. C., Campuzano-Jost, P., Jimenez, J. L., McDuffie, E. E., Fibiger, D. L., Veres, P. R., Brown, S. S., Campos, T. L., Weinheimer, A. J., Flocke, F. F., Norris, G., O'Mara, K., Green, J. R., Fiddler, M. N., Bililign, S., Shah, V., Jaegle, L., and Thornton, J. A.: Airborne observations of reactive inorganic chlorine and bromine species in the exhaust of coal-fired power plants, J. Geophys. Res. Atmos., 123, 11 225–11 237, https://doi.org/10.1029/2018JD029284, 2018.

Li, Q., Zhang, L., Wang, T., Tham, Y. J., Ahmadov, R., Xue, L., Zhang, Q., and Zheng, J.: Impacts of heterogeneous uptake of dinitrogen pentoxide and chlorine activation on ozone and reactive nitrogen partitioning: Improvement and application of the WRF-Chem model in southern China, Atmos. Chem. Phy., 16, 14 875–14 890, https://doi.org/10.5194/acp-16-14875-2016, 2016.

Liao, J., Sihler, H., Huey, L. G., Neuman, J. A., Tanner, D. J., Friess, U., Platt, U., Flocke, F. M., Orlando, J. J., Shepson, P. B., Beine, H. J., Weinheimer, A. J., Sjostedt, S. J., Nowak, J. B., Knapp, D. J., Staebler, R. M., Zheng, W., Sander, R., Hall, S. R., and Ullmann, K.: A comparison of Arctic BrO measurements by chemical ionization mass spectrometry and long path-differential optical absorption spectroscopy, J. Geophys. Res. Atmos., 116, D00R02, https://doi.org/10.1029/2010JD014788, 2011.

Liao, J., Huey, L. G., Tanner, D. J., Flocke, F. M., Orlando, J. J., Neuman, J. A., Nowak, J. B., Weinheimer, A. J., Hall, S. R., Smith, J. N., Fried, A., Staebler, R. M., Wang, Y., Koo, J. H., Cantrell, C. A., Weibring, P., Walega, J., Knapp, D. J., Shepson, P. B., and Stephens,

C. R.: Observations of inorganic bromine (HOBr, BrO, and Br_2) speciation at Barrow, Alaska, in spring 2009, J. Geophys. Res. Atmos., 117, D00R16, https://doi.org/10.1029/2011JD016641, 2012.

Liao, J., Huey, L. G., Liu, Z., Tanner, D. J., Cantrell, C. A., Orlando, J. J., Flocke, F. M., Shepson, P. B., Weinheimer, A. J., Hall, S. R., Ullmann, K., Beine, H. J., Wang, Y., Ingall, E. D., Stephens, C. R., Hornbrook, R. S., Apel, E. C., Riemer, D., Fried, A., Mauldin, R. L., Smith, J. N., Staebler, R. M., Neuman, J. A., and Nowak, J. B.: High levels of molecular chlorine in the Arctic atmosphere, Nat. Geosci., 7, 91–94, https://doi.org/10.1038/ngeo2046, 2014.

Liu, X., Qu, H., Huey, L. G., Wang, Y., Sjostedt, S., Zeng, L., Lu, K., Wu, Y., Hu, M., Shao, M., Zhu, T., and Zhang, Y.: High Levels of Daytime Molecular Chlorine and Nitryl Chloride at a Rural Site on the North China Plain, Environ. Sci. Technol., 51, 9588–9595, https://doi.org/10.1021/acs.est.7b03039, 2017.

McDuffie, E. E., Fibiger, D. L., Dubé, W. P., Lopez-Hilfiker, F., Lee, B. H., Thornton, J. A., Shah, V., Jaeglé, L., Guo, H., Weber, R. J., Michael Reeves, J., Weinheimer, A. J., Schroder, J. C., Campuzano-Jost, P., Jimenez, J. L., Dibb, J. E., Veres, P., Ebben, C., Sparks, T. L., Wooldridge, P. J., Cohen, R. C., Hornbrook, R. S., Apel, E. C., Campos, T., Hall, S. R., Ullmann, K., and Brown, S. S.: Heterogeneous N_2O_5 uptake during winter: Aircraft measurements during the 2015 WINTER campaign and critical evaluation of current parameterizations, J. Geophys. Res. Atmos., 123, 4345–4372, https://doi.org/10.1002/2018JD028336, 2018.

McNeill, V. F., Patterson, J., Wolfe, G. M., and Thornton, J. A.: The effect of varying levels of surfactant on the reactive uptake of N_2O_5 to aqueous aerosol, Atmos. Chem. Phy., 6, 1635–1644, https://doi.org/10.5194/acp-6-1635-2006, 2006.

Mielke, L. H., Furgeson, A., and Osthoff, H. D.: Observation of $ClNO_2$ in a mid-continental urban environment, Environ. Sci. Technol., 45, 8889–96, https://doi.org/10.1021/es201955u, http://www.ncbi.nlm.nih.gov/pubmed/21877701, 2011.

Müller, M., Mikoviny, T., Feil, S., Haidacher, S., Hanel, G., Hartungen, E., Jordan, A., Märk, L., Mutschlechner, P., Schottkowsky, R., Sulzer, P., Crawford, J. H., and Wisthaler, A.: A compact PTR-ToF-MS instrument for airborne measurements of volatile organic compounds at high spatiotemporal resolution, Atmospheric Meas. Tech., 7, 3763–3772, https://doi.org/10.5194/amt-7-3763-2014, 2014.

Nault, B. A., Campuzano-Jost, P., Day, D. A., Schroder, J. C., Anderson, B., Beyersdorf, A. J., Blake, D. R., Brune, W. H., Choi, Y., Corr, C. A., de Gouw, J. A., Dibb, J., DiGangi, J. P., Diskin, G. S., Fried, A., Huey, L. G., Kim, M. J., Knote, C. J., Lamb, K. D., Lee, T., Park, T., Pusede, S. E., Scheuer, E., Thornhill, K. L., Woo, J.-H., and Jimenez, J. L.: Secondary Organic Aerosol Production from Local Emissions Dominates the Organic Aerosol Budget over Seoul, South Korea, during KORUS-AQ, Atmos. Chem. Phy. Discuss., https://doi.org/10.5194/acp-2018-838, https://www.atmos-chem-phys-discuss.net/acp-2018-838/, 2018.

Neumann, B., Vafeidis, A. T., Zimmermann, J., and Nicholls, R. J.: Future coastal population growth and exposure to sea-level rise and coastal flooding - A global assessment, PLoS ONE, 10, https://doi.org/10.1371/journal.pone.0118571, 2015.

Osthoff, H. D., Roberts, J. M., Ravishankara, A. R., Williams, E. J., Lerner, B. M., Sommariva, R., Bates, T. S., Coffman, D., Quinn, P. K., Dibb, J. E., Stark, H., Burkholder, J. B., Talukdar, R. K., Meagher, J., Fehsenfeld, F. C., and Brown, S. S.: High levels of nitryl chloride in the polluted subtropical marine boundary layer, Nat. Geosci., 1, 324–328, https://doi.org/10.1038/ngeo177, http://www.nature.com/doifinder/10.1038/ngeo177, 2008.

Osthoff, H. D., Odame-ankrah, C. A., Tokarek, T. W., Taha, Y. M., and Corinne, L.: Low Levels of Nitryl Chloride in the Lower Fraser Valley of British Columbia, Atmos. Chem. Phy., 18, 6293–6315, https://doi.org/http://doi.org/10.5194/acp-18-6293-2018, 2014.

Reff, A., Bhave, P. V., Simon, H., Pace, T. G., Pouliot, G. A., Mobley, J. D., and Houyoux, M.: Emissions Inventory of PM2.5 Trace Elements across the United States, Environ. Sci. Technol., 43, 5790–5796, https://doi.org/10.1021/es802930x, http://pubs.acs.org/doi/abs/10.1021/es802930x, 2009.

Riedel, T. P., Bertram, T. H., Crisp, T. A., Williams, E. J., Lerner, B. M., Vlasenko, A., Li, S. M., Gilman, J., De Gouw, J., Bon, D. M., Wagner, N. L., Brown, S. S., and Thornton, J. A.: Nitryl chloride and molecular chlorine in the coastal marine boundary layer, Environ. Sci. Technol., 46, 10 463–10 470, https://doi.org/10.1021/es204632r, 2012.

Riedel, T. P., Wolfe, G. M., Danas, K. T., Gilman, J. B., Kuster, W. C., Bon, D. M., Vlasenko, A., Williams, E. J., Lerner, B. M., Veres, P. R., Roberts, J. M., Holloway, J. S., Lefer, B., Brown, S. S., and Thornton, J. A.: An mcm modeling study of nitryl chloride ($ClNO_2$) impacts on oxidation, ozone production and nitrogen oxide partitioning in polluted continental outflow, Atmos. Chem. Phy., 14, 3789–3800, https://doi.org/10.5194/acp-14-3789-2014, 2014.

Roberts, J. M., Osthoff, H. D., Brown, S. S., and Ravishankara, A. R.: N_2O_5 oxidizes chloride to Cl_2 in acidic atmospheric aerosol, Science, 321, 1059, https://doi.org/10.1126/science.1158777, 2008.

Rossi, M. J.: Heterogeneous Reactions on Salts, Chem. Rev., 103, 4823–4882, https://doi.org/10.1021/cr020507n, 2003.

Sarwar, G., Simon, H., Bhave, P., and Yarwood, G.: Examining the impact of heterogeneous nitryl chloride production on air quality across the United States, Atmos. Chem. Phy., 12, 6455–6473, https://doi.org/10.5194/acp-12-6455-2012, 2012.

Sarwar, G., Simon, H., Xing, J., and Mathur, R.: Importance of tropospheric $ClNO_2$ chemistry across the Northern Hemisphere, Geophys. Res. Lett., 41, 4050–4058, https://doi.org/10.1002/2014GL059962, 2014.

Schweitzer, F., Mirabel, P., and George, C.: Multiphase Chemistry of N_2O_5, $ClNO_2$, and $BrNO_2$, J. Phys. Chem. A, 102, 3942 – 3952, https://doi.org/10.1021/jp980748s, 1998.

Sherwen, T., Schmidt, J. A., Evans, M. J., Carpenter, L. J., Großmann, K., Eastham, S. D., Jacob, D. J., Dix, B., Koenig, T. K., Sinreich, R., Ortega, I., Volkamer, R., Saiz-Lopez, A., Prados-Roman, C., Mahajan, A. S., and Ordóñez, C.: Global impacts of tropospheric halogens (Cl, Br, I) on oxidants and composition in GEOS-Chem, Atmos. Chem. Phy., 16, 12 239–12 271, https://doi.org/10.5194/acp-16-12239-2016, 2016.

Sherwen, T., Evans, M. J., Sommariva, R., Hollis, L. D., Ball, S. M., Monks, P. S., Reed, C., Carpenter, L. J., Lee, J. D., Forster, G., Bandy, B., Reeves, C. E., and Bloss, W. J.: Effects of halogens on European air-quality, Faraday Dicuss., 200, 75–100, https://doi.org/10.1039/c7fd00026j, 2017.

Shetter, R. E. and Müller, M.: Photolysis frequency measurements using actinic flux spectroradiometry during the PEM-Tropics mission: Instrumentation description and some results , J. Geophys. Res. Atmos., 104, 5647–5661, https://doi.org/10.1029/98JD01381, 1999.

Simon, H., Kimura, Y., McGaughey, G., Allen, D. T., Brown, S. S., Osthoff, H. D., Roberts, J. M., Byun, D., and Lee, D.: Modeling the impact of $ClNO_2$ on ozone formation in the Houston area, J. Geophys. Res., 114, D00F03, https://doi.org/10.1029/2008JD010732, http://doi.wiley.com/10.1029/2008JD010732, 2009.

Slusher, D. L., Huey, L. G., Tanner, D. J., Flocke, F. M., and Roberts, J. M.: A thermal dissociation - Chemical ionization mass spectrometry (TD-CIMS) technique for the simultaneous measurement of peroxyacyl nitrates and dinitrogen pentoxide, J. Geophys. Res., 109, D19 315, https://doi.org/10.1029/2004JD004670, 2004.

Stull, R. B.: An introduction to boundary layer meteorology, vol. 13, Dordrecht; Boston : Kluwer Academic Publishers, 1988.

Sullivan, J. T., McGee, T. J., Sumnicht, G. K., Twigg, L. W., and Hoff, R. M.: A mobile differential absorption lidar to measure sub-hourly fluctuation of tropospheric ozone profiles in the Baltimore-Washington, D.C. region, Atmospheric Meas. Tech., 7, 3529–3548, https://doi.org/10.5194/amt-7-3529-2014, 2014.

Tanaka, P. L., Oldfield, S., Neece, J. D., Mullins, C. B., and Allen, D. T.: Anthropogenic sources of chlorine and ozone formation in urban atmospheres, Environ. Sci. Technol., 34, 4470–4473, https://doi.org/10.1021/es991380v, 2000.

Tanaka, P. L., Riemer, D. D., Chang, S., Yarwood, G., McDonald-Buller, E. C., Apel, E. C., Orlando, J. J., Silva, P. J., Jimenez, J. L., Canagaratna, M. R., Neece, J. D., Mullins, C. B., and Allen, D. T.: Direct evidence for chlorine-enhanced urban ozone formation in Houston, Texas, Atmos. Environ., 37, 1393–1400, https://doi.org/10.1016/S1352-2310(02)01007-5, 2003.

Thaler, R. D., Mielke, L. H., and Osthoff, H. D.: Quantification of nitryl chloride at part per trillion mixing ratios by thermal dissociation cavity ring-down spectroscopy, Anal. Chem., 83, 2761–2766, https://doi.org/10.1021/ac200055z, 2011.

Tham, Y. J., Wang, Z., Li, Q., Yun, H., Wang, W., Wang, X., Xue, L., Lu, K., Ma, N., Bohn, B., Li, X., Kecorius, S., Größ, J., Shao, M., Wiedensohler, A., Zhang, Y., and Wang, T.: Significant concentrations of nitryl chloride sustained in the morning: Investigations of the causes and impacts on ozone production in a polluted region of northern China, Atmos. Chem. Phy., 16, 14 959–14 977, https://doi.org/10.5194/acp-16-14959-2016, 2016.

Thornton, J. A., Braban, C. F., and Abbatt, J. P. D.: N_2O_5 hydrolysis on sub-micron organic aerosols: the effect of relative humidity, particle phase, and particle size, Phys. Chem. Chem. Phys., 5, 4593–4603, https://doi.org/10.1039/b307498f, http://xlink.rsc.org/?DOI=b307498f, 2003.

Thornton, J. A., Kercher, J. P., Riedel, T. P., Wagner, N. L., Cozic, J., Holloway, J. S., Dubé, W. P., Wolfe, G. M., Quinn, P. K., Middlebrook, A. M., Alexander, B., and Brown, S. S.: A large atomic chlorine source inferred from mid-continental reactive nitrogen chemistry, Nature, 464, 271–274, https://doi.org/10.1038/nature08905, http://www.nature.com/doifinder/10.1038/nature08905, 2010.

Wang, T., Tham, Y. J., Xue, L., Li, Q., Zha, Q., Wang, Z., Poon, S. C. N., Dubé, W. P., Blake, D. R., Louie, P. K. K., Luk, C. W. Y., Tsui, W., and Brown, S. S.: Observations of nitryl chloride and modeling its source and effect on ozone in the planetary boundary layer of southern China, J. Geophys. Res. Atmos., 121, 2476–2489, https://doi.org/10.1002/2015JD024556.Received, 2016.

Wang, X., Wang, H., Xue, L., Wang, T., Wang, L., Gu, R., Wang, W., Tham, Y. J., Wang, Z., Yang, L., Chen, J., and Wang, W.: Observations of N_2O_5 and $ClNO_2$ at a polluted urban surface site in North China: High N_2O_5 uptake coefficients and low $ClNO_2$ product yields, Atmos. Environ., 156, 125–134, https://doi.org/10.1016/j.atmosenv.2017.02.035, 2017.

Wayne, R. P., Barnes, I., Biggs, P., Burrows, J. P., Canosa-Mas, C. E., Hjorth, J., Le Bras, G., Moortgat, G. K., Perner, D., Poulet, G., Restelli, G., and Sidebottom, H.: The nitrate radical: Physics, chemistry, and the atmosphere, Atmos. Environ., 25, 1–203, https://doi.org/10.1016/0960-1686(91)90192-A, 1991.

Weinheimer, A. J., Walega, J. G., Ridley, B. A., Gary, B. L., Blake, D. R., Blake, N. J., Rowland, F. S., Sachse, G. W., Anderson, B. E., and Collins, J. E.: Meridional distributions of NO_x, NO_y, and other species in the lower stratosphere and upper troposphere during AASE II, Geophys. Res. Lett., 21, 2583–2586, https://doi.org/10.1029/94GL01897, 1994.

Wolfe, G. M., Marvin, M. R., Roberts, S. J., Travis, K. R., and Liao, J.: The framework for 0-D atmospheric modeling (F0AM) v3.1, Geosci. Model Dev., 9, 3309–3319, https://doi.org/10.5194/gmd-9-3309-2016, 2016.

Woodcock, A. H.: Salt Nuclei in Marine Air As a Function of Altitude and Wind Force, J. Meteorol., 10, 362–371, https://doi.org/10.1175/1520-0469(1953)010<0366:SNIMAA>2.0.CO;2, http://journals.ametsoc.org/doi/abs/10.1175/1520-0469%281953%29010%3C0366%3ASNIMAA%3E2.0.CO%3B2, 1953.

Young, C. J., Washenfelder, R. A., Edwards, P. M., Parrish, D. D., Gilman, J. B., Kuster, W. C., Mielke, L. H., Osthoff, H. D., Tsai, C., Pikelnaya, O., Stutz, J., Veres, P. R., Roberts, J. M., Griffith, S., Dusanter, S., Stevens, P. S., Flynn, J., Grossberg, N., Lefer, B., Holloway, J. S., Peischl, J., Ryerson, T. B., Atlas, E. L., Blake, D. R., and Brown, S. S.: Chlorine as a primary radical: Evaluation of methods to understand its role in initiation of oxidative cycles, Atmos. Chem. Phy., 14, 3427–3440, https://doi.org/10.5194/acp-14-3427-2014, 2014.

Atmos. Chem. Phys. Discuss., https://doi.org/10.5194/acp-2018-1216
Manuscript under review for journal Atmos. Chem. Phys.
Discussion started: 27 November 2018

Atmospheric Chemistry and Physics Discussions

Table 1. Summary of the measurements carried out during the KORUS-AQ 2016 field campaign, used in this study.

Compound	Method		
	TRF	OP	DC-8
NO	[a]CL	[b]FRM	[c]CL
NO_2	[d]CRDS	[e]CAPS	[c]CL
O_3	[f]DIAL	[g]SL-UV	[c]CL
SO_2	[h]PF	[i]UV florescence	x
CO	[j]IR	[k]NDIR	x
$ClNO_2$,Cl_2	[l]CIMS	[l]CIMS	[l]CIMS
VOCs	[m]PTR-ToF-MS	[o]QCL	[p]PTR-ToF-MS
	[n]TILDAS		[q]WAS
chloride	x		
nitrate	x	[r]ToF-AMS	[s]HR-ToF-AMS
sulfate	x		
surface area (< 200 *nm*)	x	x	[t]SMPS
surface area (200 *nm* - 5 μm)	x	x	[u]LAS
Jvalues	x	x	[v]CAFS

[a]Chemiluminescence with a molybdenum converter (Thermo Scientific 42i - TL), [b]Chemiluminescence detector (Federal Reference Method, Teledyne T200U), [c]NCAR 4-channel chemiluminesecence (Weinheimer et al., 1994), [d]Cavity Ring Down Spectroscopy (Los Gatos Research NO_2 analyzer), [e]Cavity Attenuated Phase Shift spectroscopy (Teledyne T500U CAPS analyzer), [f]NASA TROPospheric OZone DIfferential Absorption Lidar (Sullivan et al., 2014), [g]UV photometric method (2B 211), [h]Pulsed fluorescence method (Thermo Scientific 43i-HL), [i]UV florescence method (KENTEK), [j]Infrared CO analyzer (Thermo Scientific 48i-HL), [k]Non-Dispersive Infrared CO analyzer (KENTEK), [l]Chemical Ionization Mass Spectrometer (Slusher et al., 2004), [m]Proton-Transfer-Reaction Time-of-Flight Mass Spectrometer (IONICON), [n]Tunable Infrared Laser Direct Absorption Spectroscopy (Aerodyne), [o]Quantum Cascade Laser spectrometer (Aerodyne), [p]University of Oslo/Innsbruck Proton-Transfer-Reaction Time-Of-Flight Mass Spectrometer (Müller et al., 2014), [q]Whole Air Sampler (Colman et al., 2001), [r]Aerosol Mass Spectrometer (Aerodyne), [s]University of Colorado, Boulder,Aerosol Mass Spectrometer (Nault et al., 2018), [t]NASA, Scanning Mobility Particle Sizer, [u]NASA, Laser Aerosol Spectrometer, [v]NCAR, Charged-coupled device Actinic Flux Spectroradiometers (Shetter and Müller, 1999)

Atmos. Chem. Phys. Discuss., https://doi.org/10.5194/acp-2018-1216
Manuscript under review for journal Atmos. Chem. Phys.
Discussion started: 27 November 2018

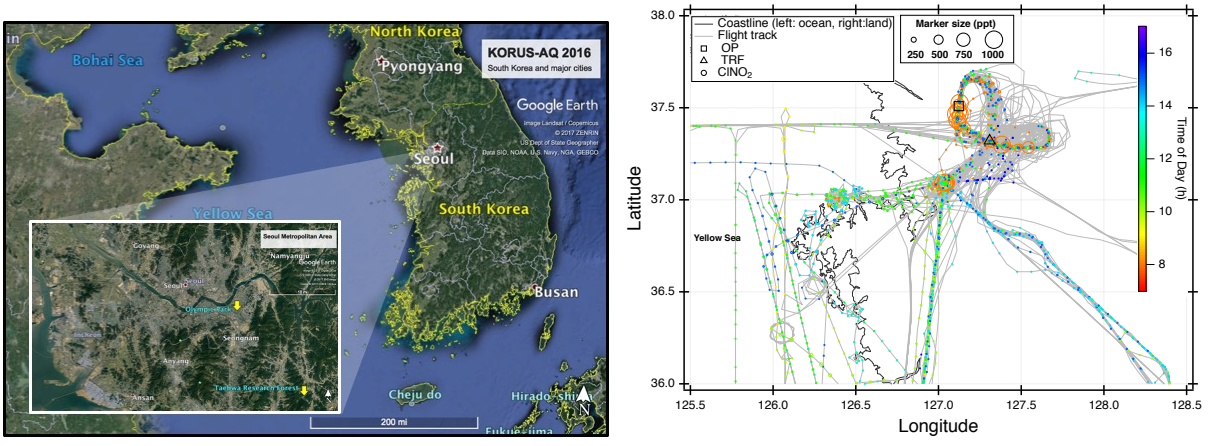

Figure 1. (a) Location of two ground sites (Taehwa Research Forest and Olympic Park) where the chemical ionization mass spectrometry (CIMS) was installed during the KORUS-AQ 2016 field campaign (b) Airborne measurements of $ClNO_2$ and DC-8 flight tracks during the whole campaign. The $ClNO_2$ data points are 60 sec averaged and color coded by time of day of the measurement. The marker size is proportional to the mixing ratio of $ClNO_2$.

Atmos. Chem. Phys. Discuss., https://doi.org/10.5194/acp-2018-1216
Manuscript under review for journal Atmos. Chem. Phys.
Discussion started: 27 November 2018

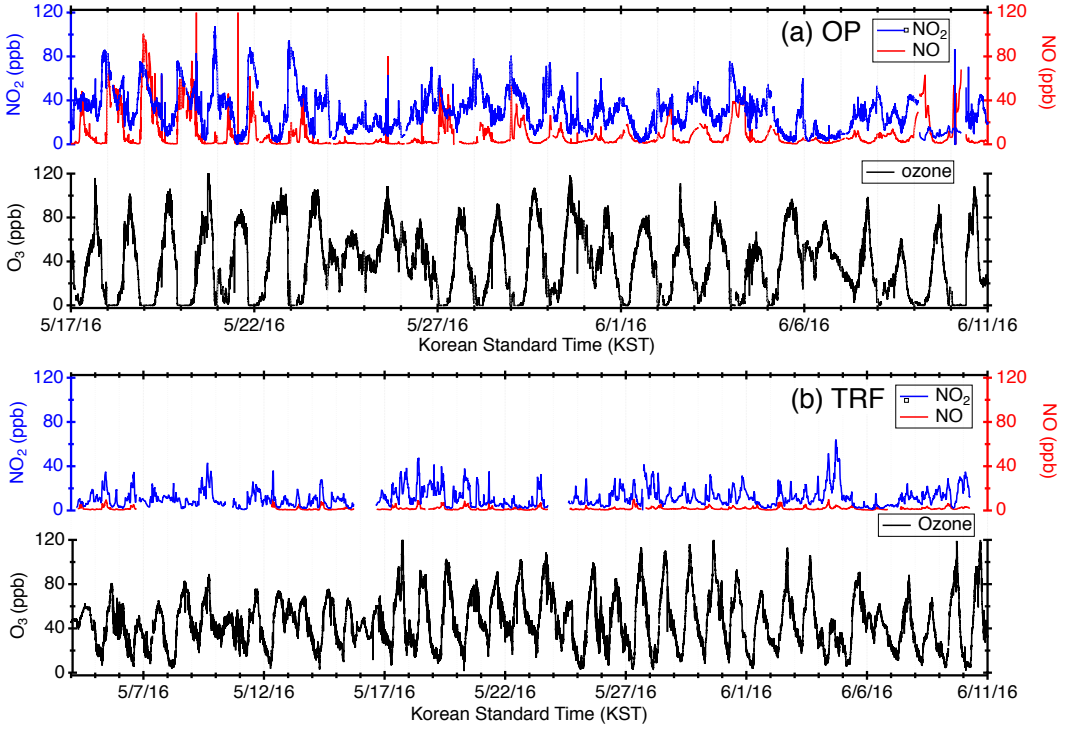

Figure 2. Temporal variation of trace gases measured at the (a) Olympic Park site (OP) and (b) Taehwa Research Forest (TRF). For the measurements at OP, the frequency of the averaged data is 1 min for NO_x and O_3. For the TRF, it was 10 min for NO_x and 1 min for O_3.

Atmos. Chem. Phys. Discuss., https://doi.org/10.5194/acp-2018-1216
Manuscript under review for journal Atmos. Chem. Phys.
Discussion started: 27 November 2018

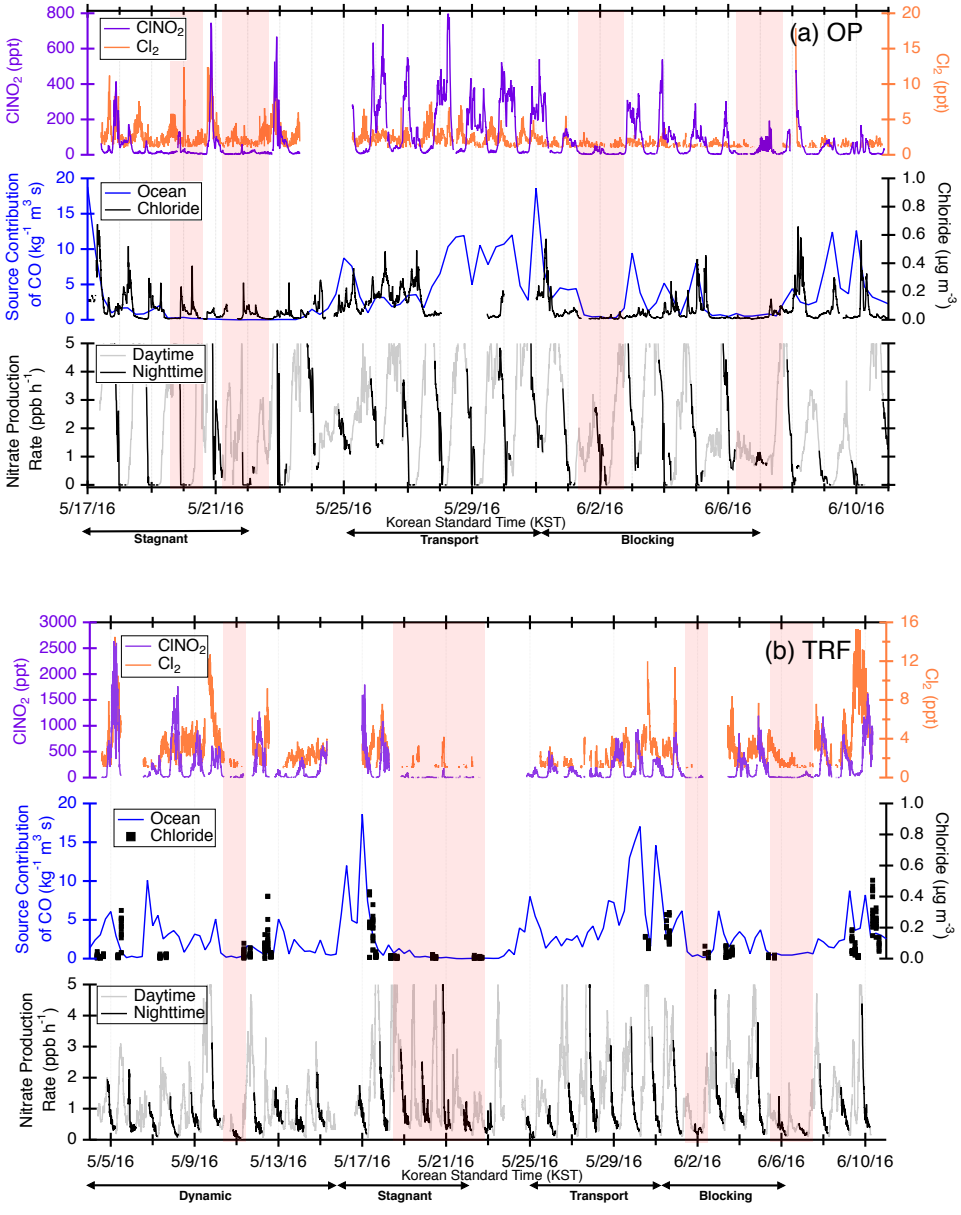

Figure 3. $ClNO_2$ and Cl_2 observation results at (a) OP and (b) TRF averaged over 10 min and 5 min respectively. FLEXPART back trajectory analysis were made for source contribution of CO-like substance originating from the ocean, assuming inert CO. Calculations were driven by WRF with a 5 km grid and each release were initiated from the ground sites for every 6 hours and followed for 5 days back in time. Aerosol chloride mass concentration (ambient μg m^{-3})) was measured at the ground for the OP site and on the NASA DC-8 in boundary layer ($<$ 1 km) over the Taehwa forest for TRF. Red shades are the time frame with limited $ClNO_2$ production.

Atmos. Chem. Phys. Discuss., https://doi.org/10.5194/acp-2018-1216
Manuscript under review for journal Atmos. Chem. Phys.
Discussion started: 27 November 2018

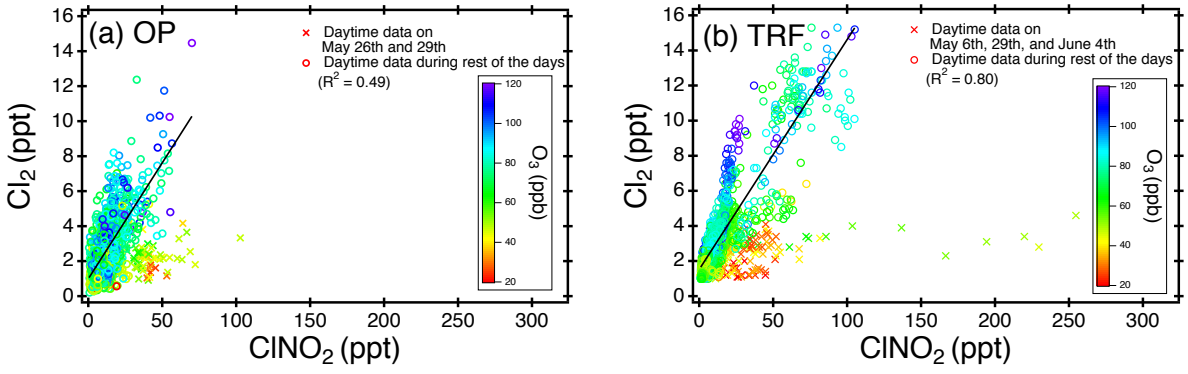

Figure 4. Scatter plot of daytime (11:00 - 18:00 local time) $ClNO_2$ and Cl_2 at (a) OP and (b)TRF, color coded with measured O_3. 5 min averaged data for the whole campaign were used for both sites.

Atmos. Chem. Phys. Discuss., https://doi.org/10.5194/acp-2018-1216
Manuscript under review for journal Atmos. Chem. Phys.
Discussion started: 27 November 2018

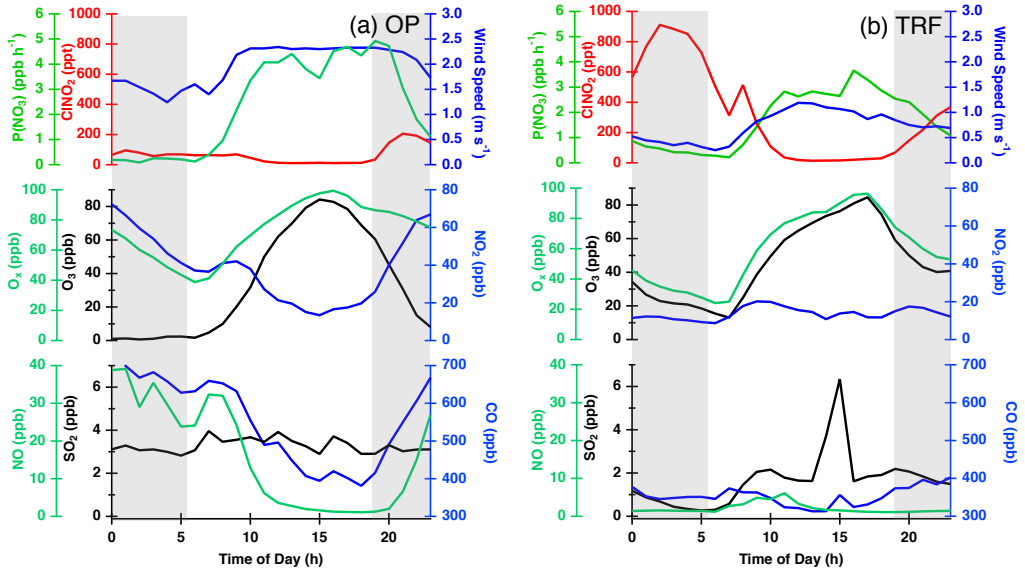

Figure 5. Diurnal variation $ClNO_2$ and other trace gases measured during the campaign and averaged over selected days at (a) OP (7 days) and (b) TRF (9 days). Night time is shown as grey shades.

Atmos. Chem. Phys. Discuss., https://doi.org/10.5194/acp-2018-1216
Manuscript under review for journal Atmos. Chem. Phys.
Discussion started: 27 November 2018

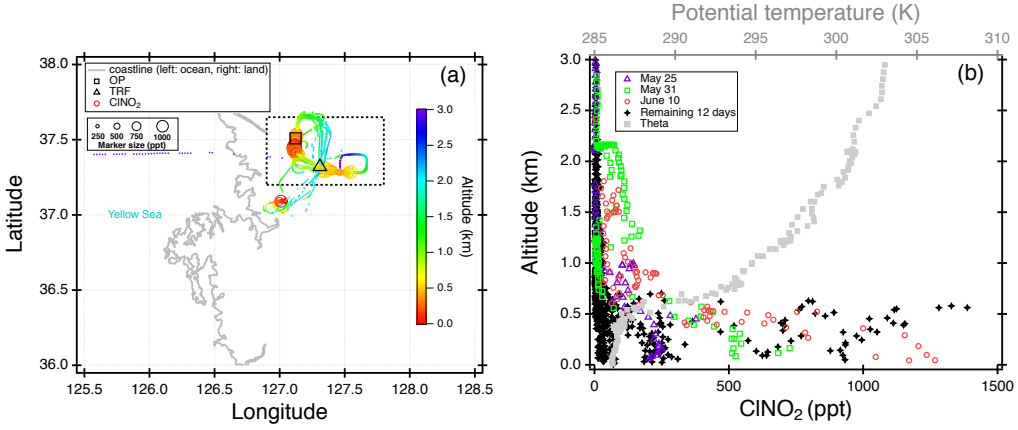

Figure 6. (a) Regional and (b) vertical distribution of airborne $ClNO_2$ measured over the Seoul Metropolitan Region (SMA) in the morning (8:00 - 8:30 local time).

Atmos. Chem. Phys. Discuss., https://doi.org/10.5194/acp-2018-1216
Manuscript under review for journal Atmos. Chem. Phys.
Discussion started: 27 November 2018

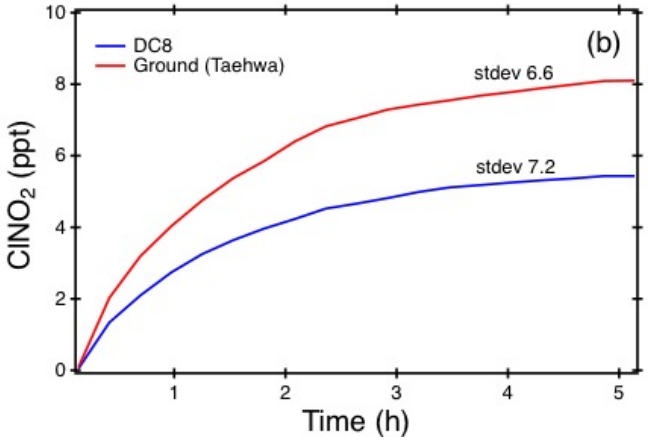

Figure 7. Box model calculated $ClNO_2$, constrained from airborne measurements (blue) and ground site data from TRF (red).

Atmos. Chem. Phys. Discuss., https://doi.org/10.5194/acp-2018-1216
Manuscript under review for journal Atmos. Chem. Phys.
Discussion started: 27 November 2018

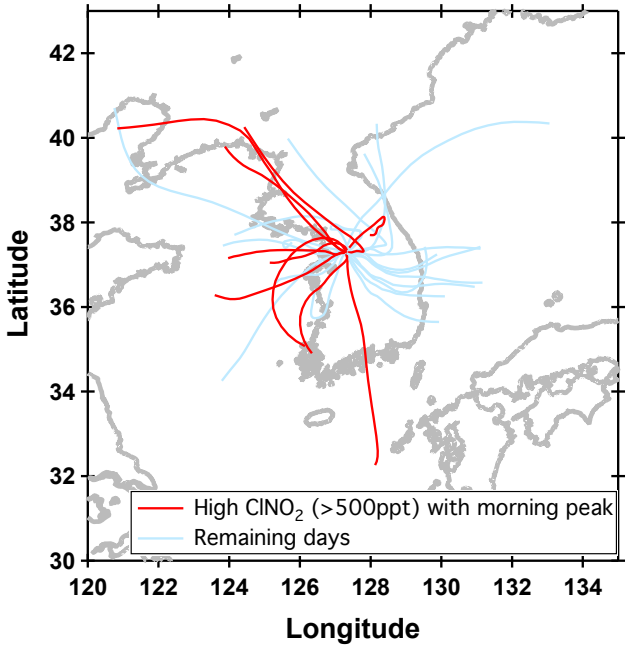

Figure 8. FLEXPART back trajectories from Taehwa Research Forest. Trajectories were initialized at 9 am local time and went 24 h backwards. Only the center trajectories with the highest percentage of airmasses are presented. Trajectories for days with high levels of $ClNO_2$ (> 500 ppt) at night are in red and the remaining days are shown in sky blue.

Atmos. Chem. Phys. Discuss., https://doi.org/10.5194/acp-2018-1216
Manuscript under review for journal Atmos. Chem. Phys.
Discussion started: 27 November 2018

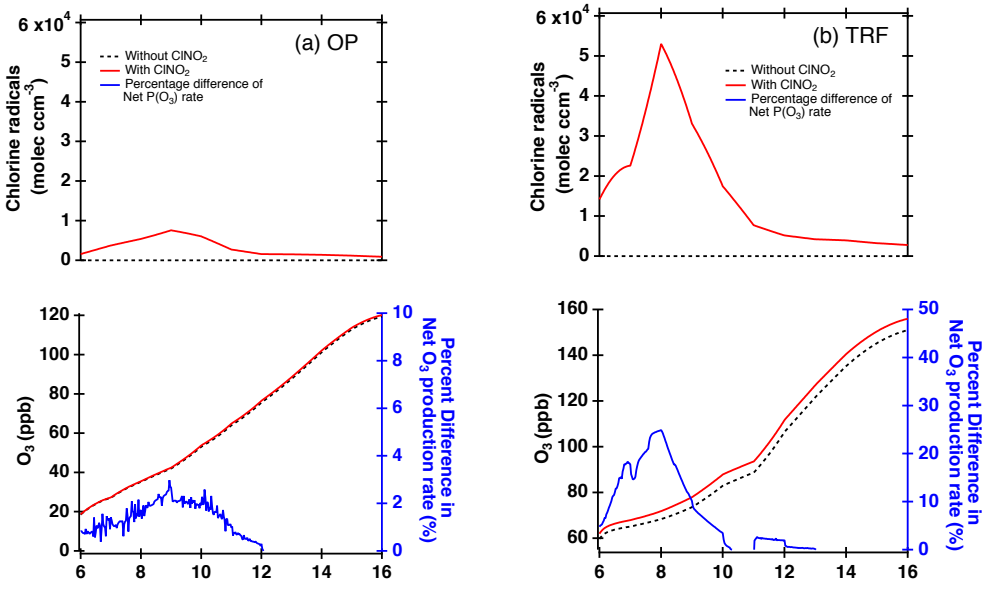

Figure 9. Box model simulations of chlorine radicals and O_3 at (a) OP and (b) TRF, constrained with $ClNO_2$ and other trace gases observed during the field campaign. Percent difference of net O_3 production rate (NetP(O_3), blue line) was calculated from the difference of the NetP(O_3) between simulations with and without $ClNO_2$ constrained in the model (i.e., 100*(w$ClNO_2$ - wo$ClNO_2$)/wo$ClNO_2$).